Available online at www.sciencedirect.com
SCIENCE DIRECT®
Nuclear Instruments and Methods in Physics Research A 512 (2003) 44–51
NUCLEAR INSTRUMENTS & METHODS IN PHYSICS RESEARCH Section A
www.elsevier.com/locate/nima

The HERMES silicon project—the radiation protection system

M.G. van Beuzekom*, O. Bouhali[1], V. Mexner, S. Mos, A. Reischl, J.J.M. Steijger

NIKHEF, P.O. Box 41882, 1009 DB Amsterdam, The Netherlands

Abstract

The HERMES-detector has recently been upgraded with a silicon detector called the Lambda Wheels. This is the first detector following the interaction region. It consists of two disks of silicon detectors close to the beamline. This location makes it vulnerable to increased radiation levels which may be caused by beam instabilities. The Lambda Wheel detector, therefore, contains a system to detect these instabilities. This additional system triggers a kicker which dumps the HERA-lepton beam when the radiation level becomes too high.

This contribution describes the radiation monitor which consists of two sets of three ionization chambers each, and the data-acquisition system which reads them out. The system has been installed and is operational since the summer of 2001. The HERA-accelerator was being commissioned after an upgrade during this time and several kinds of beam instabilities were observed with this protection system. The characteristics of some events will be described.

PACS: 87.50.N; 29.40.Wk; 29.40.C; 29.27

Keywords: Silicon strip detectors; Ionization chambers; Radiation protection; Accelerated beams

1. Introduction

The HERMES experiment has been built to study the spin structure of the nucleon. It uses the polarized positron (electron) beam of HERA, and a polarized, fixed gas target. The target consists of an open-ended storage cell in which polarized, atomic hydrogen, deuterium or ^{3}He is injected. The HERA-beam (energy 27.5 GeV, typical beam current 30 mA) is traveling along the long axis of the cell, interacting with the gas. Events are observed in a forward angle spectrometer, which covers a solid angle of ± 170 mrad horizontally, and ± 40–140 mrad vertically. A full description can be found in Ref. [1]. The experiment resulted amongst others in a precise determination of the contributions to the nucleon spin from up and down valence quarks and sea quarks [2].

The large momentum acceptance of the spectrometer and its relatively large coverage of solid angle make it possible to study a broad range of physics topics. These opportunities have been enlarged by the recent upgrades of the HERMES-detector which include a dual-radiator RICH-detector [3], and a wheel-shaped silicon detector called the Lambda Wheels [4]. This detector increases the acceptance of the spectrometer in the front region, with a view to increase

*Corresponding author. Tel.: +31-20-592-2154; fax: +31-20-592-5155.

E-mail address: martinb@nikhef.nl (M.G. van Beuzekom).

[1] Current address: Université Libre Bruxelles CP230, Boulevard du Triomphe, Bruxelles B-1050, Belgium.

0168-9002/03/$ - see front matter © 2003 Elsevier B.V. All rights reserved.
doi:10.1016/S0168-9002(03)01875-8

the fraction of Λ^0, Λ_c^+, and J/Ψ-particles which can be reconstructed.

The Lambda Wheels consist of two sets of silicon detectors in the shape of disks mounted 45 and 50 cm downstream of the centre of the target. The diameter of the disks is 33.6 cm. A central hole with a diameter of 9.2 cm leaves the space necessary for the beam and the wakefield suppressor which surrounds it. This detector is both closest to the beam in radial distance and nearest to the interaction region, which makes it vulnerable to increased radiation levels which may be caused by beam instabilities. The most sensitive elements are the electronic read-out chips in the front end, which are located furthest away at the outer periphery of the detector. We have, therefore, added to the Lambda Wheel detector a system to identify and monitor these instabilities. This Beam Loss Monitor (BLM) system is described in the following sections.

In Section 2, the details of the HERA beam structure are summarized. The design of the BLM and its calibration is described in detail in Sections 3 and 4. Finally, in Section 5 some event classes which have been observed with the BLM, and which cause an increased radiation level, are discussed.

2. The HERA-beam

The environment where the BLM has been installed is 140 cm downstream of the interaction point (the centre of the storage cell) of the HERMES-experiment, which is built around the HERA-positron ring. The proton machine, which is also part of the HERA-complex, is 71.4 cm away from the centreline of the positron ring in the horizontal plane and parallel to it. The positron ring has a circumference of 6336 m [5]. The beam is injected from the PETRA synchrotron into the HERA ring with an energy of 12 GeV and, subsequently, ramped up to an energy of 27.5 GeV. The bunches are separated in time by 96 ns, and the revolution period is 21.13 μs. In the ring, there is room for 220 bunches of which 189 are used in running conditions. In the examples shown in this contribution, only a few (3 or 5) bunches were present in the machine due to the commissioning of the HERA luminosity upgrade [5].

3. The BLM

The sensitive elements of the BLM can be any radiation sensitive detector. Cherenkov radiation detectors [6], PIN diodes [7] and ionization chambers [8] have been used for this purpose. The photomultiplier-based detectors need a very good screening of the magnetic field from the main spectrometer, and the diodes require an elaborate electronics system to separate the very temperature-dependent leakage currents from the current induced by the radiation. Ionization chambers are established, simple and reliable detectors for the measurement of radiation levels. Although they are not the most sensitive kind of detectors, they are linear over a large dynamic range which makes them suitable for the current application.

3.1. The ionization chambers

The BLM consists of two sets of three ionization chambers positioned in the horizontal plane, one on either side of the beam pipe. In line with the three chambers a fourth chamber (called dummy) is installed which lacks the gas volume of the sensitive detectors and serves as a probe for electromagnetic pick-up. The four chambers in one set all have the same electronics, and share a single high voltage connection. Signals from the dummy detector are used to veto triggers originating from environmental noise.

Fig. 1 shows the schematic representation of the ionization chambers. Each chamber is constructed from a small block ($4 \times 4 \times 1$ cm^3) of halogen-free polystyrene. In the centre of the block, a hole with a diameter of 2 cm is cut which is the active gas volume of the detector. The volume is closed on the top and bottom side by printed circuit boards with circular electrodes. The side view (bottom part of Fig. 1) shows the assembly of the ionization chamber. The bottom printed circuit board supplies the high voltage to the chamber.

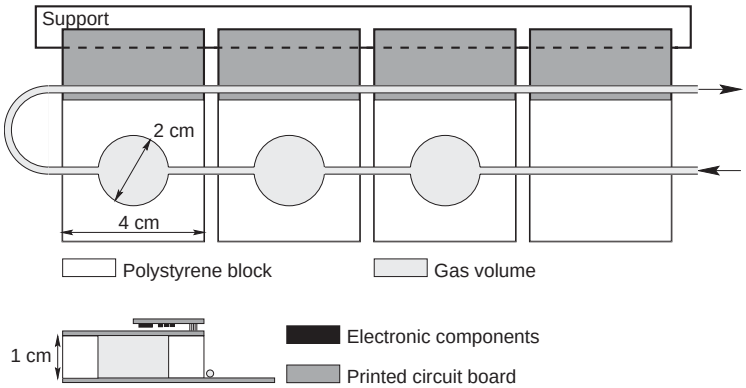

Fig. 1. Schematic diagram of the ionization chambers, showing the top view and the side view of the setup.

On top of the polystyrene, the printed circuit board with the collecting electrode is mounted that serves as a carrier for the piggy back with the front-end electronics. This facilitates a fast exchange of the non-radiation-hard front-end electronics in case of failure.

A common gas line is used for the four chambers providing a flow of argon with a rate of 1 l h^{-1}. One detector set of the type shown in Fig. 1 is positioned at the left, and another at the right-hand side of the beamline, respectively. The chambers are oriented in the horizontal plane at right angles to the beam. The centre of the first chamber is located 6 cm from the beam.

3.2. Data acquisition

The front-end electronics consists of an integrating preamplifier with a decay time constant of about 5 μs. With this time constant, time structures within the 21 μs (see Section 2) beam revolution time can be seen, but signals coming from single bunches cannot be traced back to the proper bunch. A differential line driver sends the analog signals over a 30-m-long cable from the front-end electronics to the counting room where the rest of the trigger electronics is located. A simplified diagram of the electronics is shown in Fig. 2. The signal processing electronics of the BLM is housed in a three-unit-wide NIM module. The analog signal from the front end is fed into the line receiver whereafter it is replicated three times to be measured by an ADC, and for use in the fast and the integrating trigger circuitry, respectively.

The signal for the fast non-integrating trigger is first discriminated against a threshold. Threshold levels can be set in a range from 0 to 500 mGy s^{-1}. Next, the discriminated signal should meet a certain time-over-threshold value to increase the immunity against spurious signals. This is achieved by a group of three monostable multivibrators as shown in Fig. 2. The minimum width of the discriminated signal that passes the time-over-threshold discriminator is set by the combination of CT1 and RT1. The minimum width can be set between 1 and 10 μs.

The second trigger is formed by integrating the output of the ionization chamber with a time constant of 1 s, and compare the result with a threshold. This level can be set in the range 0–0.2 or 0–1 Gy. The range can be selected during the setup of the BLM.

To be able to analyze the cause of a trigger that led to the dump of the HERA lepton beam the analog signals from the eight front ends are digitized. A PCI-ADC with 16 bit resolution continuously samples the analog signal at a rate of 1.3 MHz and stores them in a circular buffer. Upon receipt of a dump trigger, the samples corresponding to an adjustable time window (set from 47.5 ms before to 50 ms after the trigger) are written to file together with a time stamp from the local computer clock.

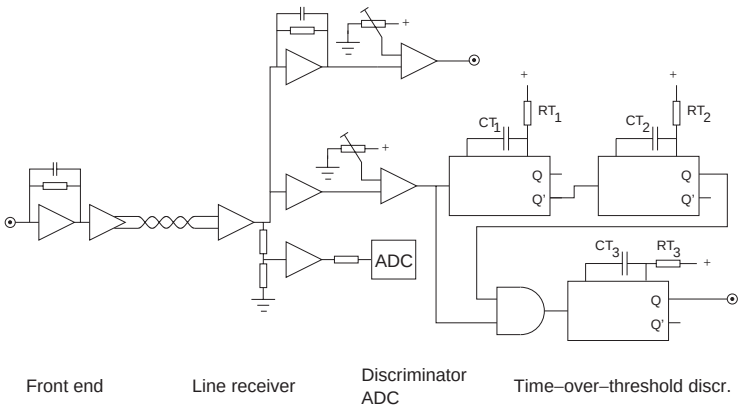

Fig. 2. Functional diagram of the electronics of the BLM showing the front-end electronics and the backend signal processing of a single channel.

3.3. Trigger logic

The final trigger decision is a four-fold logic OR-function of the signals from the left- and right-hand side of the BLM, and the fast and integrating trigger signals. A trigger from one side of the BLM consists of three signals from active detectors and a corresponding veto signal derived from the dummy chamber. A majority of active signals (two out of three) from one detector set in the absence of a veto fires the dump trigger. To allow injection of the beam in HERA which is accompanied by high radiation levels in the experiment (see Section 5.1), the BLM trigger is disabled during this time.

The dump trigger signal is sent to the lepton beam kicker which is located at the opposite side of the HERA ring, near the West experimental Hall.[2] The connection over a distance of about 4 km uses $\frac{50}{125}$ optical fibre that is driven by an optical transceiver at a wavelength of 1300 nm.

4. Calibration

The ionization chambers of the BLM were calibrated using an X-ray source. The X-ray generator was a Philips PW2773/00 tube equipped with a copper anode. A detailed description of the setup can be found in Ref. [9]. During calibration the BLM chambers were operated at 250 V, which is well above the saturation voltage of around 50 V. The calibration was performed by measuring the ionization current which is a direct measure of the ionization produced, and therefore of the absorbed dose

$$I\,t = \frac{Dm}{W}. \tag{1}$$

Here I is the ionization current, t is the collection time of the absorbed dose D, m is the mass of the argon in the chamber and W the average energy needed to produce one electron–ion pair. By scanning the X-ray beam across the chambers the size of the sensitive volume of the chamber was verified, and a small difference between the height of the sensitive volume and the geometrical height was found.

When the X-ray tube was operated at a current of 1 mA, an ionization current of 2.34 nA was observed. Using this result with Eq. (1) the calibration constant is determined

$$\dot{D} = 4.27\,I \tag{2}$$

where $\dot{D}$ is the dose rate in Gy s^{-1} and I the ionization current in μA. The dose delivered by the X-ray tube to the ionization chamber is therefore 10 mGy s^{-1}. An independent measurement of the beam intensity was made by irradiating thermoluminescence dosimeters (TLD). The measured dose equivalent is 13 mSv s^{-1}. From this result, and the known spectrum of the X-rays, the

[2] The HERMES experiment is located in the East Hall.

energy absorbed in the gas is estimated to be 8 mGy s^{-1}, which is in reasonable agreement with the result obtained from the measurement of the ionization current. The ionization current measurement is probably the more accurate, therefore the calibration we will use is that of Eq. (2). All details of the calibration can be found in Ref. [10].

5. High radiation events

In this section, some events in HERA are described that generated a high radiation level. These events illustrate the wide range of radiation levels and timescales that are covered by these incidents.

5.1. Injection in the positron machine

The orbit and size of the beam during the injection process is different from the stable closed orbit which is present during normal operation. The deviations and the beam-size are larger during this time, which results in small extra losses and higher radiation levels. Fig. 3 shows an example of the response of the BLM during an injection. The output of the BLM is sampled every 0.768 μs, but the data shown are smoothed to show the development of the radiation level at the millisecond scale. An approximately exponential decay with a time-constant of about 5 ms is observed. The flat response in the first 2 ms is due to saturation of the front-end amplifiers. The second panel in this figure shows a detail at full time-resolution. The machine was being filled with only three bunches at the time, which causes the gap between the current pulses to be large enough to be observed with the BLM which has a time constant of 5 μs. The pulses are observed at the correct time separation of 21.13 μs (see Section 2).

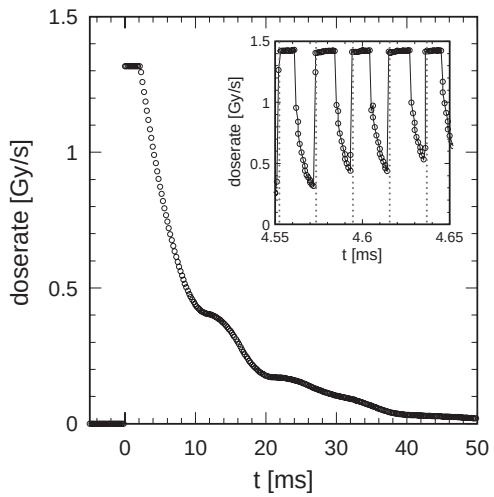

Fig. 3. Rate of absorbed dose in the BLM during the injection of beam in the HERA-positron ring. The data are smoothed, the insert shows the full (time) resolution. The vertical lines in the insert mark the consecutive revolutions of the same bunch.

5.2. Injection in the proton machine

Similar to the positron machine, also the proton machine is a source of radiation when a beam is injected into it. The proton-beampipe is some distance away from that of the positron ring, around which the ionization chambers of the BLM are positioned, but part of this radiation will still be detected. Fig. 4 shows the response of the BLM to a typical proton injection event. The amplitude of the radiation flashes is much smaller, and the duration is much shorter than that caused by injections in the positron machine. By combining

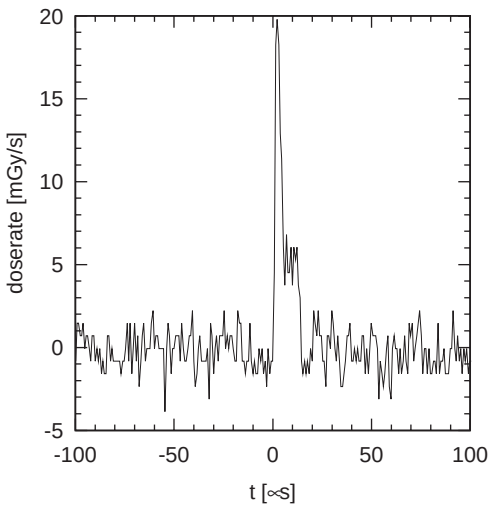

Fig. 4. Rate of absorbed dose in the BLM during the injection of beam in the proton ring.

the information from the amplitude- and time-over-threshold discriminator it is possible to prevent the triggering of the lepton kicker by proton injection.

5.3. Unexpected beam losses

The circulating beam in the storage ring is occasionally lost due to equipment malfunction, or other reasons. This loss of beam causes the high radiation levels which may damage experimental equipment, and thus forms the raison d'être for the BLM. Thereby it also supplies the signal on the basis of which the BLM decides to trigger the kicker, and dump the lepton beam intentionally. Beam losses can be caused by many different reasons, e.g. errors in the magnet power supplies, the RF-system, or the control system. The development of the radiation levels depends on the particular error causing the beam loss, the location of the affected equipment and the position of the BLM. In this paragraph a few examples of this type of events are given.

Fig. 5 shows an example of an event in which the beam was lost almost completely in one revolution. In this case, the dose rate shows a high peak, with a very short decay (300 μs), followed by a radiation tail with a much lower intensity and a longer decay (2.5 ms). The BLM has too little time to dump the beam in this case, and thus offers no protection if the beam loss occurs in the neighbourhood of the HERMES experimental area.

The second class of events is characterized by the longer time the high radiation level persists, or, alternatively, it takes to lose the beam completely. Fig. 6 shows a typical event in this class. The high radiation level persists for a few milliseconds, and falls off with a time constant of about 3 ms. This is long compared to the rise time of the kicker (about 0.5 ms); therefore, the BLM is able to dump the beam and reduce the radiation dose caused by this type of events. Unfortunately, no unambiguous cause for these events was found.

The timescales of the two previous incidents differ by about three orders of magnitude, but do not exhaust the range of possibilities. Fig. 7 shows a period of 100 ms out of the history of an event which took in total about 30 s. The intensity of the radiation is moderate, but the increased level is present for a longer time, which results in a large integrated dose. In this particular case, the beam was lost because the current in the main dipoles

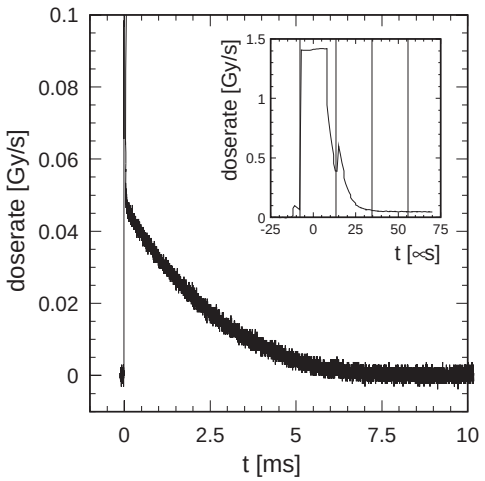

Fig. 5. Rate of absorbed dose in the BLM during an unexpected beam loss. The beam is lost almost completely in one revolution, causing a high peak in the absorbed dose (see inset), followed by a longer tail. The vertical lines in the inset mark the revolutions of the beam in the storage ring.

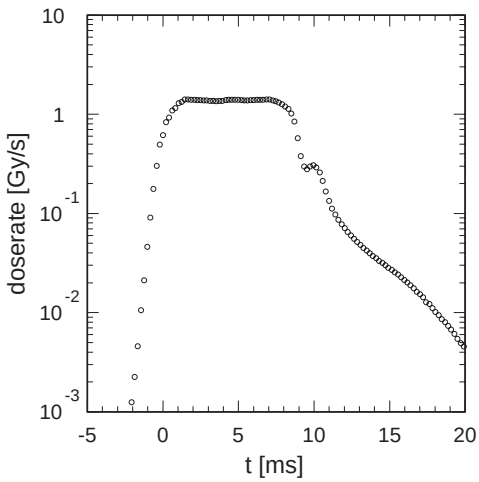

Fig. 6. Rate of absorbed dose in the BLM during an unexpected beam loss. The beam is lost in a few milliseconds, causing a high peak in the absorbed dose which decays with a time-constant of 3 ms.

dropped. This type of events will activate the integrating trigger of the BLM.

5.4. Beam instabilities

High-radiation episodes do not always culminate in the loss of beam. Their duration can be very short, in the millisecond range, or very long, in the range of hours. The range of absorbed doses varies similarly. The data shown in Fig. 8 are smoothed to show the long-term behaviour. The signal contains the same fast time structure as that presented in the inset of Fig. 3 which demonstrates that the signal originates from radiation and not from electromagnetic pick-up.

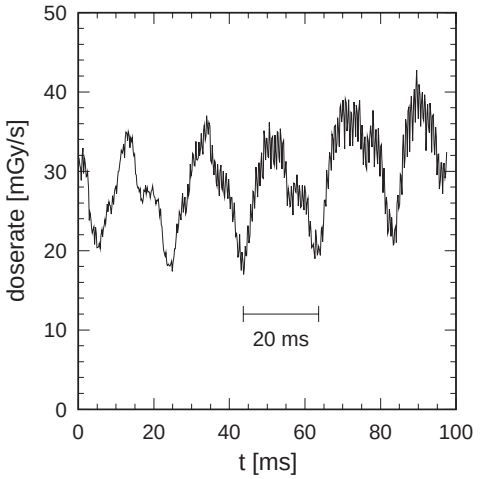

Fig. 7. Rate of absorbed dose in the BLM during an unexpected beam loss. The beam is lost in about 30 s, causing a high absorbed dose which is modulated with 50 Hz noise in this case.

6. Conclusion

The events shown in the previous section can be arranged in three groups. The first group is that of the sudden beam losses in a single revolution. The BLM cannot protect the experiment against events in this category. The second group contains beam losses which take in the order of a few milliseconds. In this case, the fast trigger of the BLM causes the beam to be kicked out of the machine, preventing a large part of the radiation to the experimental equipment. The third group is characterized by much lower peaks in the dose rate, accompanied by a much longer time. This includes *slow* beam losses and instabilities of the beam without loss. The radiation load of the experiment can still be large. The amplitude of the BLM signal is similar to that caused by the transient instabilities as shown in the left-hand panel of Fig. 8, but since the total dose in this case is not large, this should not give rise to a trigger to the kicker. A slow integrator is necessary to distinguish these two event types.

Acknowledgements

The HERMES silicon project is a collaboration between the University of Erlangen-Nürnberg, the

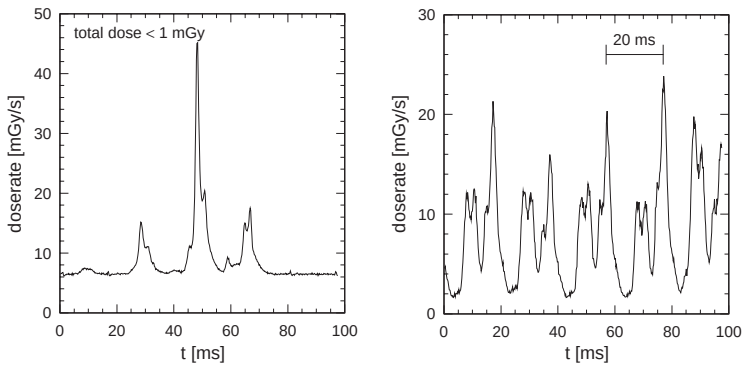

Fig. 8. Rate of absorbed dose in the BLM in periods associated with beam instabilities. Left-hand panel: transient which occurred during tuning of the beam for luminosity conditions. Right-hand panel: this condition lasted for several hours, the radiation is modulated with a 50 Hz noise.

PNPI, St Petersburg, Vrije Universiteit and NIKHEF. We are grateful to the group of prof. Ph. Herquet, faculté des sciences, université de Mons-Hainaut, who allowed the use of their X-ray generator for the calibration. In particular, the hospitality and help of Evelyne Daubie, Francis Defontaines and Isabelle Boulogne is acknowledged. This work was supported in part by the Stichting voor Fundamenteel Onderzoek der Materie (FOM), which is financially supported by the Nederlandse Organisatie voor Wetenschappelijk Onderzoek (NWO).

References

[1] K. Ackerstaff, et al., Nucl. Instr. and Meth. A 417 (1998) 230.
[2] K. Ackerstaff, et al., Phys. Lett. B 464 (1999) 123.
[3] N. Akopov, et al., Nucl. Instr. and Meth. A 479 (2002) 511.
[4] M.G. van Beuzekom, et al., Nucl. Instr. and Meth. A 461 (2001) 247.
[5] U. Schneekloth (Ed.), The HERA luminosity upgrade, Technical Report HERA 98-05, Deutsches Elektronen-Synchrotron DESY, 1998.
[6] T. Kawakubo, et al., Fast response beam loss monitor, in: Proceedings of the 15th Meeting of the International Collaboration on Advanced Neutron Sources, Vol. 1, Japan Atomic Energy Research Institute, 2001, p. 299.
[7] K. Wittenburg, et al., Experience with the electron and proton beam loss monitor (BLM) systems at HERA, in: Fifth European Particle Accelerator Conference, Vol. 2, Institute of Physics Publishing, Bristol, 1997, p. 1612.
[8] R. Witkover, et al., RHIC beam loss monitor system design, in: Proceedings of the 1997 Particle Accelerator Conference, Vol. 2, IEEE, Piscataway, NJ, USA, 1998, p. 2218.
[9] I. Boulogne, et al., Study of X-rays produced by a generator equipped with a copper target using a single wire proportional chamber, Technical Report UMH PNPE#344, Universite de Mons-Hainaut, 1999.
[10] O. Bouhali, et al., Test of the HERMES beam loss monitor with X-rays, Technical Report HERMES 01-054, HERMES-collaboration, 2001.